Experimental Design of a Joule-Thomson Cryocooler for Mixture Optimization of a Mixed-Gas Joule-Thomson Cycle

J. Detlor, J. Pfotenhauer, and G. Nellis

University of Wisconsin-Madison, Department of Mechanical Engineering
Madison, WI 53706, USA

ABSTRACT

This study expands on prior research by further developing a computational tool designed to optimize the gas mixture composition for a Joule-Thomson (JT) cryocooler with specific operating parameters. The mixture optimization model determines an optimal three-component mixture based on the analysis of the maximum value of the minimum isothermal enthalpy change, Δh_T, that occurs over the operating temperature range coupled with an evaluation of the percent of the heat exchanger that exists in a two-phase range. Other performance metrics such as cooling load, coefficient of performance and heat exchanger conductance were subsequently considered during the final mixture selection.

In addition, initial design work to experimentally validate the tool is described. A prototype JT cryocooler has been constructed and is being installed in a test facility capable of providing a range of gas compositions, flow rates, and pressures. The prototype has been designed to enable easy access to the JT expansion orifice, minimize cooldown time, and minimize the parasitic heat load due to conduction.

INTRODUCTION

Joule-Thomson (JT) cycles can be used in many applications, ranging from cryosurgery to low temperature cooling of sensors. JT cycles are less efficient than Stirling cycle cryocoolers; however, the cooling capacity of JT cycles for a given overall size of the device can be larger than other cycles. Research has shown that using a suitable mixed gas fluid can provide an increased cooling capability while operating at lower pressures and pressure ratios than is possible with a pure fluid.[1] However, properly selecting a suitable mixture is a challenging design problem as is decreasing the overall size of the device. A MATLAB program was previously developed to determine an optimal three-component mixture based on the analysis of the maximum value of the minimum Δh_T.[2,3] The program has been improved, and work has started that will allow us to experimentally validate the modeling results through the assembly of a JT cryocooler prototype.

MIXTURE OPTIMIZATION MODEL

A MATLAB program was previously developed to determine an optimal three-component mixture based on the analysis of the maximum value of the minimum Δh_T that occurs for each

Cryocoolers 20, edited by S.D. Miller, R.G. Ross, Jr. and J.R. Raab
©International Cryocooler Conference, Inc., Boulder, CO, 2018

mixture given a relatively large list of candidate fluids with a fixed load and supply temperatures and fixed suction and discharge pressures. This was accomplished using three nested functions: the outer, intermediate, and inner functions. The outer function returns tables of optimal compositions and maximum values of the minimum Δh_T that occur for all of the three-component mixtures analyzed. The intermediate function uses nested loops to run through a range of possible molar compositions for the three-component mixture passed from the outer function. The inner function returns the minimum Δh_T that occurs for a specified composition of the three-component mixture passed from the intermediate function.[2]

Further development of the inner function has focused on outlier detection and thermodynamic consistency of enthalpy data. These developments more accurately assess the maximum value of the minimum Δh_T that occurs for mixtures that include outlier values of enthalpy returned from the property routine REFPROP and therefore increase confidence that values of enthalpy being removed from vectors of data returned directly from REFPROP are truly outliers.[4] Additionally, the mixture optimization model was updated to calculate additional performance metrics such as cooling load and *COP* for mixtures that showed the greatest refrigeration effect for the cycle parameters.

Outlier Detection

Previous Model. As shown in Fig. 1, large discontinuities in the enthalpy data are evident for a given specified three-component mixture during the analysis of the minimum Δh_T that occurs over a range of temperatures. The large discontinuities are due to issues of convergence within the property routine REFPROP. In previous versions of the mixture optimization model, values of enthalpy were considered to be outliers if the enthalpy was greater than 2.5 to 4 standard deviations from the median value of enthalpy for the high and low pressure stream. Enthalpy data marked as outliers were then removed, along with their corresponding temperature, from the temporary vectors storing the pressure stream data.

This method of determining outliers did not always provide the best results. For example, when a low value of standard deviation was chosen as the filter then the enthalpy data corresponding to the limits of the analyzed temperature range might be identified as outliers and removed. This would occur even if the enthalpy data at the minimum or maximum values of the temperature range did not visually appear to be outliers. Removal of these values of enthalpy and their corresponding temperatures would misleadingly restrict the analyzed mixture to a smaller temperature. On the other hand, when a larger value of standard deviation was chosen as the method of assessing

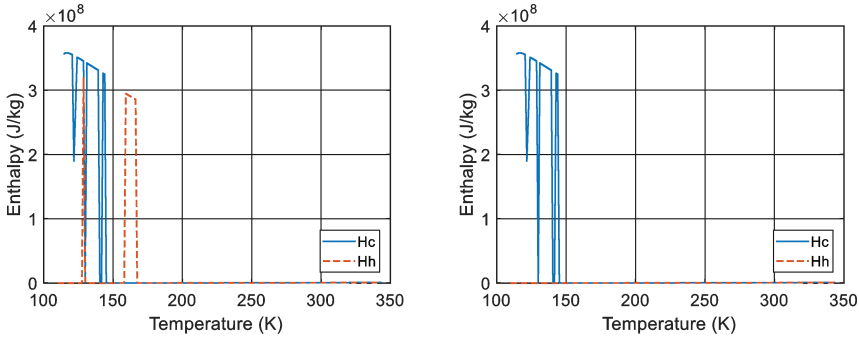

Figure 1. Visualization of outlier detection used by the inner function by the previous version of the model when outliers were determined as values greater than 4 standard deviations from the median value of enthalpy. Shown is the raw enthalpy data returned from REFPROP (left) and enthalpy data stored after outliers had been removed (right). Hh and Hc are the enthalpies for the hot and cold (high and low pressure) streams, respectively. The specific example shown is for 10% nitrogen, 72% ethane and 18% pentane at a load temperature of 150 K with suction and discharge pressure of 100 and 300 psi, respectively. In this case, the inner function does not return a minimum Δh_T as all values of enthalpy returned by REFPROP have been identified as being outliers and the mixture was discarded.

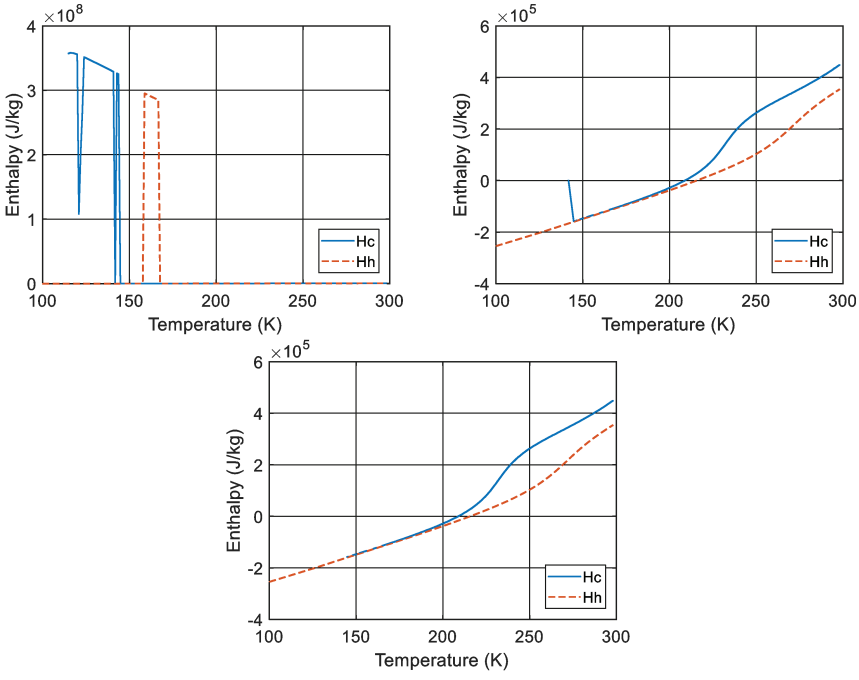

Figure 2. Visualization of the two-stage outlier detection used by the inner function in the updated version of the mixture optimization model. Shown is the raw enthalpy data (top left), the enthalpy data stored after the min/max restriction is implemented (top right), and the enthalpy data stored after isoutlier is implemented (bottom). Hh and Hc are the same as described in Fig. 1 as is the specific example shown. In this case, the inner function does return a minimum Δh_T.

outliers, then enthalpy data that visually appeared to be outliers might not be identified and removed. By retaining these values, inaccurate values of Δh_T were calculated or no minimum Δh_T was returned from the model as shown in Fig. 1.

Updated Model. The updated version of the mixture optimization model contains a two-stage outlier detection process. The first stage imposes a minimum and maximum restriction for enthalpy data to accomplish a more robust outlier detection. The second stage implements the MATLAB function isoutlier with a moving window to target local outliers. Enthalpy data greater than three scaled median absolute deviations (MAD) from the median value of enthalpy within that window are marked as outliers and removed from the data set. This method of outlier detection is more effective as the MAD is less affected than the standard deviation of a data set by extremely high or low enthalpy data. This new method of outlier detection allows us to have more confidence that the enthalpy data near the limits of the temperature range analyzed are not outliers in the pressure stream data set. Figure 2 demonstrates the two-stage method of outlier detection and its effectiveness compared to the previous method shown in Fig. 1.

Thermodynamic Consistency of Enthalpy Data

Previous Model. In previous versions of the mixture optimization model, enthalpy data that decreased with an increase in temperature for the high and low pressure streams were considered to be thermodynamically inconsistent and removed from the temporary vectors storing the pressure stream data. This would ensure that the enthalpy data in the temporary vectors was thermodynamically consistent. While this method of checking for thermodynamically consistent enthalpy data worked well for removing enthalpy data that appears as "low" outliers (i.e., values below the true enthalpy), it removed enthalpy data from the temporary vectors that were thermodynamically consistent if the enthalpy data included "high" outliers (i.e., values above the true enthalpy).

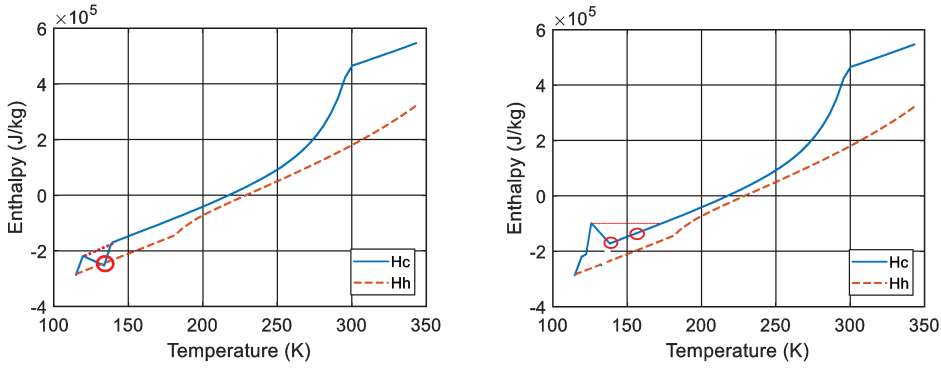

Figure 3. Visualization of the check for thermodynamically inconsistent enthalpy data for "low" (left) and "high" outliers (right) used by the inner function in the previous version of the mixture optimization model. The plot shown on the left is for a mixture of 50% methane, 45% pentane and 5% propane at a load temperature of 115K and suction and discharge pressures of 22 and 363 psi, respectively. The plot shown on the right is a theoretical rendering of a thermodynamic inconsistency that could occur. The circled data points are values of enthalpy considered thermodynamically inconsistent and removed from the data set. The bold dashed line is the trend line then interpolated by the model.

To illustrate, the enthalpy data circled in the plot on the left side of Fig. 3 is thermodynamically inconsistent as the value of enthalpy decreases with an increase in temperature. In the previous version of the mixture optimization model, this value of enthalpy would be removed from the temporary vector storing the pressure stream data and the model would then use the remaining enthalpy data to interpolate information for this temperature range. The same process would be used on the two values of enthalpy circled for the plot on the right side of Fig. 3. While this ensures that the enthalpy data in the temporary vector storing the pressure stream data is thermodynamically consistent, the enthalpy data targeted as outliers by the model in the second plot do not visually appear as outliers. In fact, the enthalpy data preceding these two points appears to be the outlier and the model would calculate a more consistent Δh_T if this enthalpy data was removed from the temporary vector storing data.

Updated Model. The updated version of model removes enthalpy data if the value of enthalpy decreases with an increase in temperature and, in addition, removes the value of enthalpy and its corresponding temperature for the previous data point analyzed. While this method of checking for thermodynamic consistency removes two values of enthalpy instead of one, there is increased confidence that the enthalpy data that is removed is actually an outlier. The enthalpy data circled in the plots of Fig. 4 are removed from the pressure stream data with the updated model. The model then uses the remaining enthalpy data to interpolate enthalpy data for this temperature range. A comparison between the enthalpy trend line of the previous and updated versions of the model can be seen by comparing the dashed lines in Fig. 3 and Fig. 4. Furthermore, it can be seen that the updated model will calculate a more consistent Δh_T.

Previous and Updated Model Comparison

The mixture optimization model has been run for both hydrocarbon and synthetic refrigerant mixtures. The mixture optimizations were performed for three sets of suction and discharge pressures: 100-300 psi, 100-400 psi, and 22-363 psi. All mixtures were investigated for load temperatures ranging from 110-180 K in increments of 10 K while the supply temperature remained constant at 343.15K. Results for all three sets of suction and discharge pressures are detailed in previously published works evaluating the refrigeration per molar flow rate as a function of load temperature, the percent of the heat exchanger that exists in a two-phase range, and the gaps in the temperature range where enthalpy data was not available from REFPROP.[2] The comparison below focuses on suction and discharge pressures of 100-300 psi as an example.

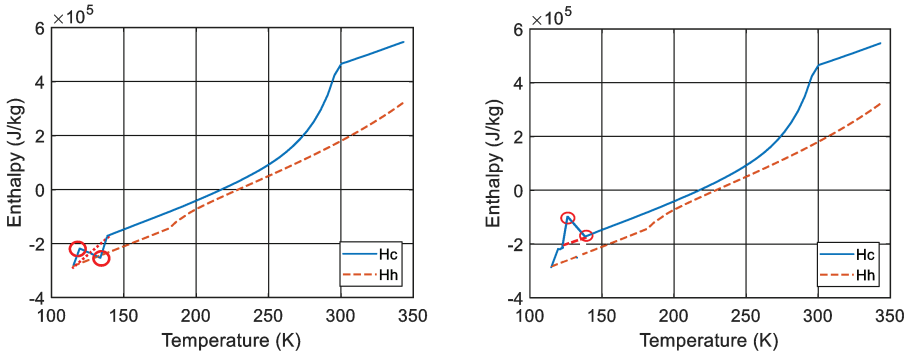

Figure 4. Visualization of the check for thermodynamically inconsistent enthalpy data for "low" (left) and "high" (right) outliers used by the inner function in the updated version of the mixture optimization model. The specific examples shown are the same as shown in Fig. 3. The circled data points are values of enthalpy considered thermodynamically inconsistent and removed from the data set. The bold dashed line is the trend line that is then interpolated by the model.

Refrigeration Per Molar Flow Rate and Maximum Temperature Gap. Shown at the top left corner of Fig. 5 is a plot comparing the refrigeration per molar flow rate, $\dot{Q}/\dot{n}$, of the previous and updated mixture optimization models for 100-300 psi. Each marker represents the optimal combination of three fluids and composition selected specifically for that load temperature. It can be seen that the previous model was overestimating the greatest value of $\dot{Q}/\dot{n}$ for load temperatures

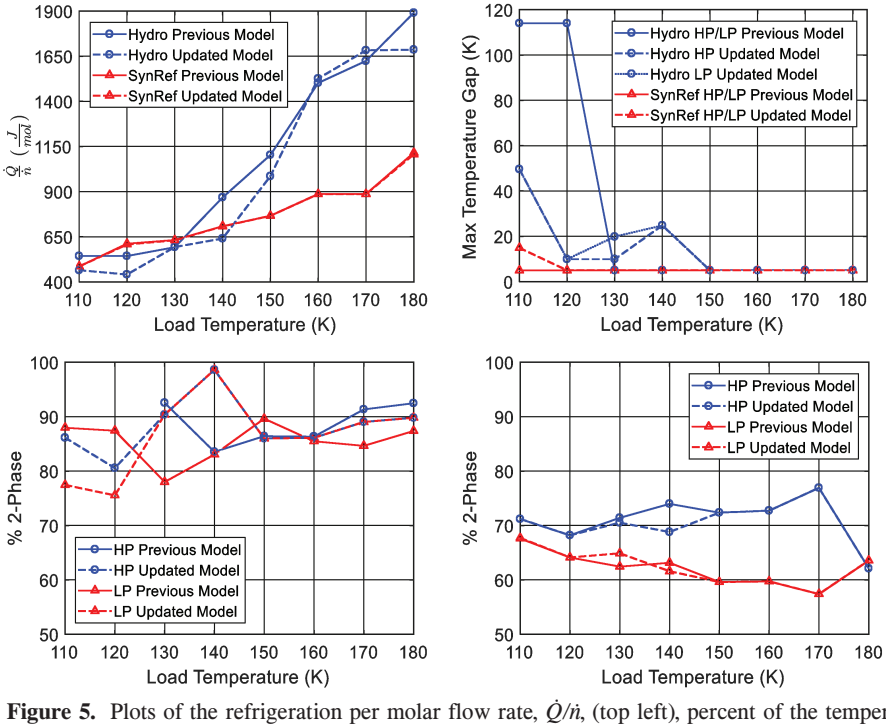

Figure 5. Plots of the refrigeration per molar flow rate, $\dot{Q}/\dot{n}$, (top left), percent of the temperature range that is two-phase for the optimal hydrocarbon (bottom left) and synthetic refrigerant (bottom right) mixtures, and maximum temperature gap (top right) as a function of the load temperature for suction and discharge pressures of 100-300 psi for the previous and updated model. Values for the high and low pressure streams (HP and LP) are shown for the percent of the temperature range that is two-phase and the maximum temperature gap.

below 160 K and above 170 K for the hydrocarbon optimal composition mixtures. For the synthetic refrigerant optimal composition mixtures, the updates to the model did not significantly affect the greatest values of $\dot{Q}/\dot{n}$ for each load temperature.

It is not surprising that the updates to the model more greatly affected the greatest values of $Q/\dot{n}$ for the optimal hydrocarbon mixtures. As shown at the top right corner of Fig. 5, the optimal hydrocarbon mixtures of the previous model had large ranges of temperature where enthalpy data was not available from REFPROP. The optimal hydrocarbon mixtures of the updated model have decreased maximum temperature gaps where enthalpy data is not available. With more enthalpy data available to analyze, the values of $\dot{Q}/\dot{n}$ are better estimated. The optimal synthetic refrigerant mixtures of the previous model consistently had a maximum temperature gap consistent with the temperature segmentation used to call REFPROP indicating the enthalpy data was consistently returned from REFPROP. The updated model did not generally affect the maximum temperature gap for the optimal synthetic refrigerants and therefore it can be seen that the greatest values of $\dot{Q}/\dot{n}$ were not significantly impacted.

Percent Two-Phase. The percent of the recuperator that is a two-phase state was calculated using the bubble and dew points for the optimal mixtures and comparing them to the load and supply temperatures. As the optimal combination and composition of hydrocarbon and synthetic refrigerant mixtures selected for each load temperature changed from the previous to the updated model, so too did the percent of the temperature range that is two-phase.

Shown on the bottom of Fig. 5 are plots comparing the percent of the temperature range that is two-phase for the optimal hydrocarbon and synthetic refrigeration mixtures for the high and low pressure streams. For the low pressure stream of the optimal hydrocarbon mixtures, the percent of the temperature range that is two-phase increased or decreased depending on mixture and load temperature. For the high pressure stream, the updated model returned values for the percent of the temperature range that is two-phase of the optimal hydrocarbon mixtures at load temperatures of 110 K and 120 K when the previous model had been unable to return the bubble and/or dew points from REFPROP for the optimal mixtures. For load temperatures above 130 K, the percent of the temperature range that is two-phase for the high pressure stream of the optimal hydrocarbon mixtures was not significantly affected by the updates. The high and low pressure streams of the optimal synthetic refrigerant mixtures were marginally affected by the updates for load temperatures of 120 K to 150 K.

Performance Parameters

The mixture optimization model was updated to evaluate the cooling load and coefficient of performance, *COP,* for mixtures with the greatest refrigeration effect for the cycle. All mixtures were analyzed for suction and discharge pressures of 50-150 psi, a molar flow rate of 0.04 mmol/s, UA of 0.25 W/K, and compressor clearance volume fraction of 0.025.

Cooling Load. As shown in Fig. 6a, the hydrocarbon optimal composition mixtures produce the greatest cooling load for all load temperatures for suction and discharge pressure of 50-150 psi. While the optimal hydrocarbon and synthetic refrigerant mixtures produce comparable cooling loads at load temperatures of 110-130 K, the optimal hydrocarbon mixtures increasingly outperform the optimal synthetic refrigerant mixtures as the load temperature increases from 140-180 K.

Coefficient of Performance. The power needed for the compressor is estimated based on the following isentropic compressor model:

$$\dot{W}_{comp} = \dot{V}\eta_v P_{suc}\left(\frac{k}{k-1}\right)\left[\left(\frac{P_{dis}}{P_{suc}}\right)^{\frac{k-1}{k}} - 1\right] \quad (1)$$

where

$$\eta_v = 1 + C - C\left(\frac{P_{dis}}{P_{suc}}\right)^{\frac{1}{k}} \quad (2)$$

is the volumetric efficiency, $\dot{V}$ is the displacement rate of the compressor, P_{suc} is the suction pressure, P_{dis} is the discharge pressure and k is the isentropic index.[5] $\dot{V}$ is calculated from the mass flow

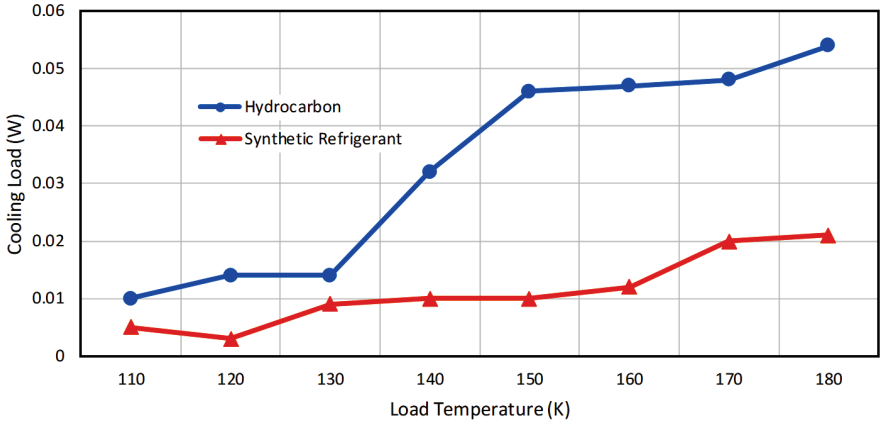

Figure 6a. Plot of the cooling load as a function of the load temperature for the optimal hydrocarbon and synthetic refrigerant mixtures with a molar flow rate of 0.04 mmol/s, supply temperature of 343.15K, pressures of 50-150 psi and UA of 0.25 W/K. Each point on the plot is a unique mixture identified by the model.

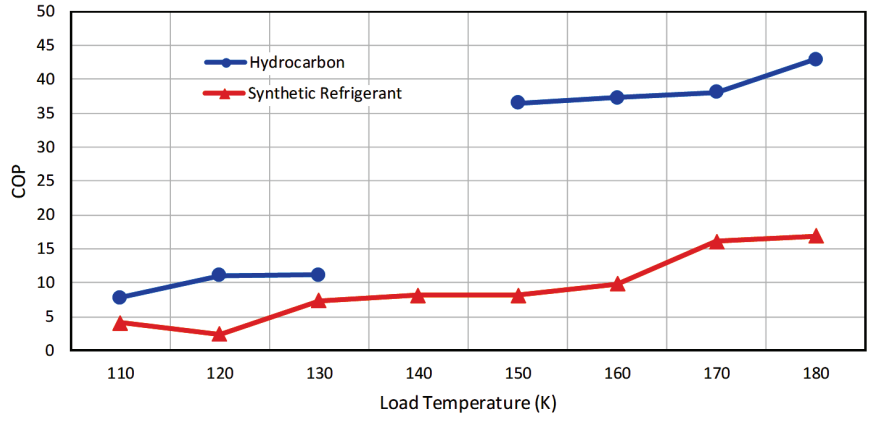

Figure 6b. Plot of *COP* as a function of the load temperature for the optimal hydrocarbon and synthetic refrigerant mixtures with a molar flow rate of 0.04 mmol/s, supply temperature of 343.15 K, pressures of 50-150 psi and UA of 0.25 W/K. Each point on the plot is a unique mixture identified by the model.

rate and density of the mixture. The *COP* is then determined from the ratio of the cooling load of the cycle to the power needed for the compressor.

As shown in Fig. 6b, the hydrocarbon optimal composition mixtures produce the greatest *COP* for suction and discharge pressure of 100-300 psi. The results for the *COP* follow the same trends as outlined for the cooling load of the cycle parameters. The value of COP could not be calculated for the optimal hydrocarbon mixture with load temperature of 150 K as the isentropic index was not returned from REFPROP.

CRYOCOOLER DESIGN

Design Overview

A SOLIDWORK CAD software rendering of the cryocooler is shown in Fig. 7 along with a picture of the assembled device. The design features a 1" VCR female nut and plug at the fluid inlet/outlet. The inlet/outlet tubing is soldered to the heat exchanger tubing and to the 1" VCR plug. The stainless steel tubing encompassing the length of the heat exchanger has an inner diameter of 0.73" and a wall thickness of 0.01". Two 1" VCR butt weld glands were shortened to a length of

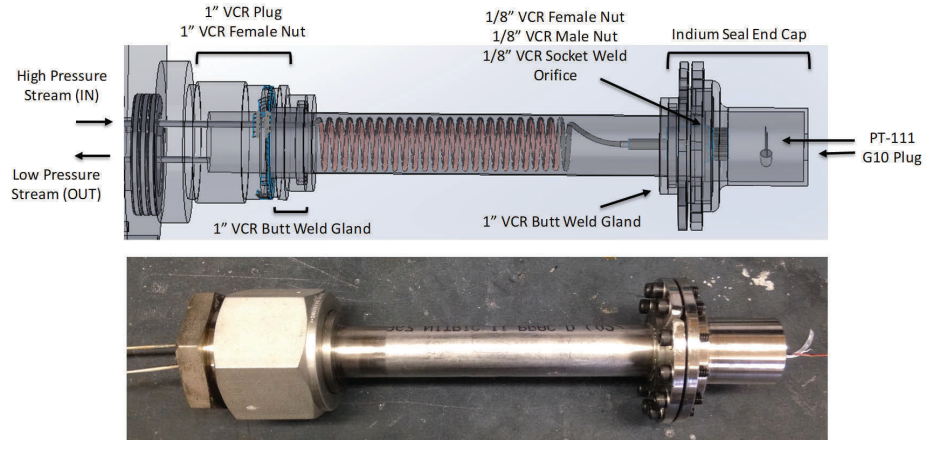

Figure 7. A SOLIDWORK CAD software rendering of the JT cryocooler prototype and a picture of the assembly are shown in the top and bottom images, respectively. Not shown for visual simplicity in the software rendering is the G-10 composite mandrel and G-10 composite end plug with PRT support structure.

0.53" and welded along with a connector to the thin-walled stainless steel tubing. The end cap surrounding the JT orifice and the fluid temperature sensor consists of a flange split into two C-pieces and nipple held together by twelve #6-32 socket head screws. A groove was machined on the inside of the end cap to allow for an indium seal. The JT orifice consists of a 1/8" copper blank with a small diameter hole in its center. The JT orifice is located at the exit of heat exchanger for the high pressure stream and is held in place by 1/8" VCR female and male nuts. The temperature sensor is secured to a G-10 composite plug which is epoxied to the end cap. The JT cryocooler measures 7.89" in overall length.

The heat exchanger shown in Fig. 7 is where the three-component mixture is cooled to the desired temperature. The heat exchanger has an outer diameter of 0.748" and a length of 3". The tube for the high pressure stream is helically wound with copper fins and has an inner and outer diameter of 0.041" and 0.056", respectively. The finned tubing is helically wound 24 times in a single-layer around a G-10 composite mandrel of 0.475" in outer diameter and 3.5" in length. The high pressure fluid enters the heat exchanger as at the bottom of the helically wound tubing as shown in Fig. 7 and leaves the heat exchanger at the JT orifice. The low pressure stream then returns to the outlet by flowing over the fins on the outside of the high pressure stream tubing. A conservative estimate of 0.25 W/K was calculated for the conductance of the heat exchanger assuming single-phase flow throughout. The actual conductance is hypothesized to be dramatically larger as the heat transfer coefficient associated with two-phase flow will be much larger than the heat transfer coefficient for single-phase flow.[6]

The prototype has been assembled and is currently being installed in a test facility capable of proving a range of gas compositions, flow rates, and pressures. The test facility consists of a compressor station, vacuum vessel, and data acquisition station. The compressor station consists of a Danfoss SC18CLX compressor capable of providing pressure ratios of up to 13:1, an Endress & Hauser Promass 83A Coriolis mass flow meter, discharge and suction tanks, oil separators, a RCW42 filter-dryer, and a Lyton tube-and-fin heat exchanger. The cryocooler assembly rests inside a vacuum vessel equipped with a Leybold D8A Trivac rotary vane pump and a Pfeifer TSU 261 turbo vacuum pump. The temperature at the exit of the JT orifice will be measured along with the flow rate and suction and discharge pressures. Data will be collected through a Campbell Scientific CR23X-TD Datalogger. Gas mixture compositions will be measured with a 5890 Series II Hewlett-Packard gas chromatograph.[6,7]

Below the areas of focus for the experimental design of the cryocooler are discussed including enabling easy access to the JT expansion orifice, minimizing cooldown time and parasitic heat load due to conduction, and facilitating accurate fluid temperature measurement.

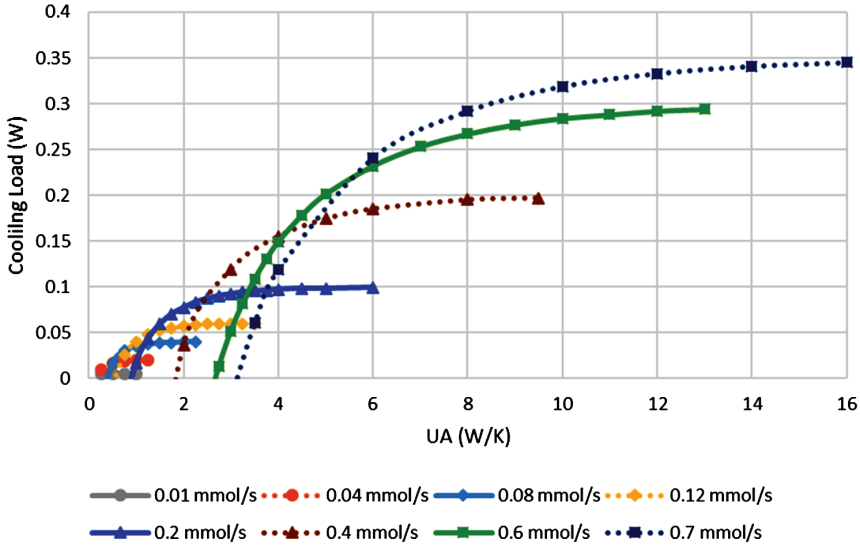

Figure 8. Plot of the cooling load as a function of conductance for various molar flow rates for the optimal refrigerant mixture at a load temperature of 130K.

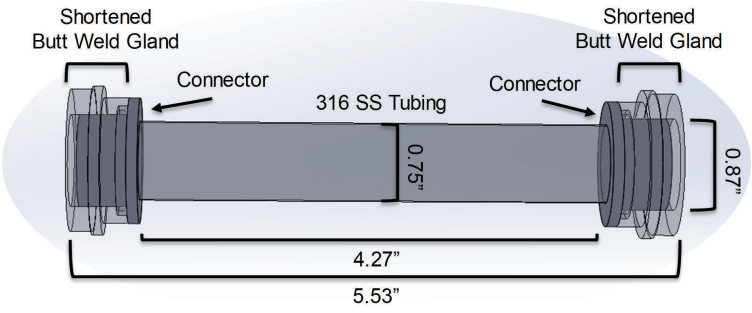

Figure 9. A SOLIDWORK CAD software rendering of the heat exchanger sleeve.

Areas of Focus for Experimental Design

Parasitic Heat Load. Figure 8 illustrates the cooling capacity of the cryocooler as a function of conductance and molar flow rate. As can be seen, the cooling capacity of the cryocooler is below 0.35 W for testing parameters greater than the targeted molar flow rate and estimated value of conductance. Therefore it was important to focus on minimizing parasitic heat loss in the cryocooler design. The design minimizes parasitic heat loss through the construction of a thin-walled stainless steel sleeve shown in Fig. 9, which encloses the heat exchanger. The sleeve is 0.75" in outer diameter and has a wall thickness of 0.01". This design reduces the parasitic heat load to an estimated value of 0.301W. The butt weld glands were retained in the design to preserve the ability to easily access the JT orifice through the end cap.

Cooldown Time. The design minimizes cooldown time and retains easy access to the JT orifice through a flange and nipple end cap design with an indium seal as shown in Fig. 10. Care was taken in the design of the end cap to reduce bolt size, wall thickness, and clearances to minimize the mass of the flange and nipple without compromising the integrity of the end cap under targeted testing pressures. The overall size of the end cap is 2.076" in outer diameter and 1.614" in

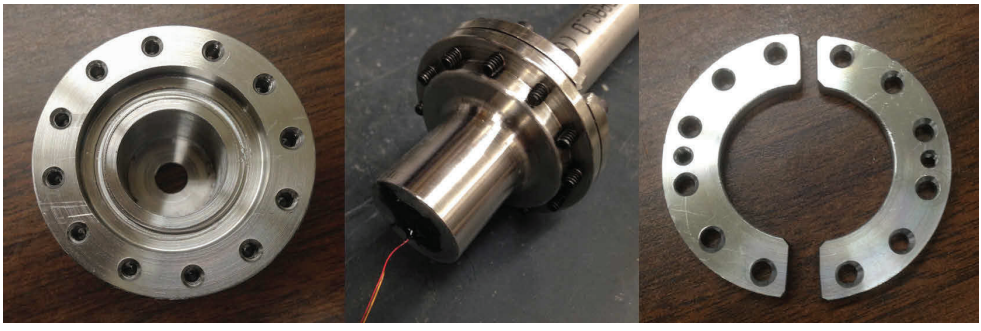

Figure 10. Images of the flange and nipple end cap design. The indium groove can be seen in the nipple (left). The additional bolt holes in the two C-pieces of the flange (right) are to make it easier to separate the nipple and flange after use of the indium seal.

height. The nipple has an inner and outer diameter of 0.86” and 0.96”, respectively, and height of 1.15”. The groove for the indium seal has an inner and outer diameter of 1.03” and 1.23”, respectively, and depth of 0.016”. The mass of the end cap was minimized to 116.9 g for an estimated cooldown time of 16.5 hours to reach 110K.

Fluid Temperature Measurement. The fluid temperature measurement sensor was chosen to be the Lake Shore Cryotronics platinum resistance thermometer (PRT) Model PT-111. The placement of the heat exchanger within the heat exchanger sleeve positioned the JT orifice inside the end cap leaving only 0.3” in height for the PRT. Therefore it was important to focus on a compressed design for the PRT and its supporting structure. The orientation of the PRT body and leads was designed in ordered for it to lay across the bottom of the nipple. The length of the PRT body and leads measures at 0.6” while the inner diameter of the nipple is 0.86”. A stainless steel support structure was bent in a manner so that it could be epoxied to the G-10 composite plug and support the PRT laying across the full length of the diameter of the nipple. The G-10 composite plug isolates the PRT from the surrounding tubing while the support structure reduces the possibility of damage to the PRT. Heat shrink wrap was placed around the support structure to ensure the thermal path of least resistance to the temperature sensor is through the PRT leads. Measurement wires were wrapped around the support structure to secure the PRT and provide a heat sink.[8] A picture of the PRT and support structure can be seen in Fig. 11. The overall length of the structure measured 0.84”. Kapton tape was wrapped around the PRT body and the measurement wires to isolate the structure from the surrounding tubing.

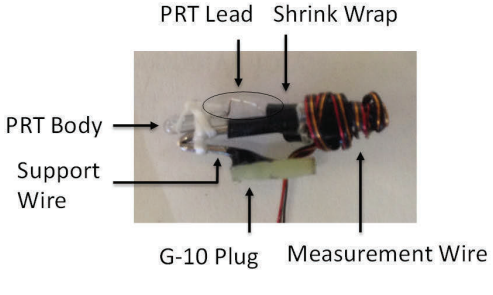

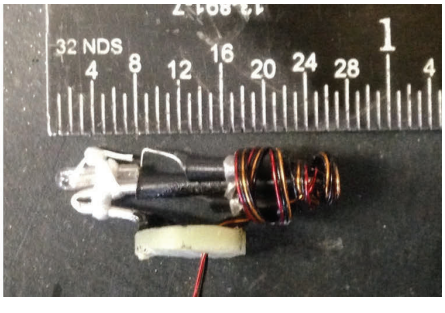

Figure 11. Images of the PRT and support structure. The assembly to secure the PRT to the support structure is detailed on the left. The size of the PRT and support structure is shown on the right.

CONCLUSION

This paper describes further development of a computational tool designed to optimize the gas mixture composition for a JT cycle with specific operating parameters as well as the design challenges faced during prototype assembly of the cryocooler. Further development of the mixture optimization model focused on outlier detection, thermodynamic consistency of enthalpy data, and the calculation of additional performance parameters. From analysis of the cooling load and *COP*, the optimal hydrocarbon mixtures appear to provide greater cooling load capacity and *COP* for the operating parameters analyzed. However, from previous work, the uncertainty that the maximum values of minimum Δh_T are accurate below 130 K for the hydrocarbon mixtures suggest that the synthetic refrigerants should still be considered.

A design overview was provided for the assembled JT cryocooler prototype. Constraints placed on the cryocooler design due to the low cooling capacity of the optimal composition mixtures and space limitations generated challenges to remove as much stainless steel mass as possible without compromising the integrity of the cryocooler. Design challenges were focused on reducing parasitic heat loss, cooldown time and size of the PRT supporting structure.

REFERENCES

1. Hinze J F, Klein S A, and Nelllis G, F.T. “Thermodynamic optimization of mixed gas refrigerant Joule-Thomson systems constrained by heat transfer considerations,” *IOP Conf. Ser: Mater. Sci. Eng*, 101 (2015) 012133.
2. Detlor J, Pfotenhauer J, and Nellis G, F.T. “Mixture optimization for mixed gas Joule-Thomson cycle,” *IOP Conf. Ser: Mater. Sci. Eng*, 278 (2017) 012045.
3. MATLAB release R2017a, The MathWorks, Inc., Natick, Massachusetts, United States.
4. Lemmon E W, Huber M L, McLinden M O. NIST Standard Reference Database 23: Reference Fluid Thermodynamic and Transport Properties-REFPROP, Version 9.1, National Institute of Standards and Technology, Standard Reference Data Program, Gaithersburg, 2013.
5. Hinze J, F.T., “Thermodynamic optimization of mixed refrigerant Joule-Thomson cycle with heat transfer considerations,” (Madison: Univ. of Wisc. Madison) MS [thesis] Available from: UW Madison Library System.
6. Barraza R, F.T. “Thermal-fluid behavior of mixed refrigerants for cryogenic applications,” (Madison: Univ. of Wisc. Madison) PhD [dissertation] Available from: UW Madison Library System.
7. Schwartz J, F.T., “Measurement of Mixed-Gas Heat Transfer Coefficients,” (Madison: Univ. of Wisc. Madison) MS [thesis] Available from: UW Madison Library System.
8. Hughes C, F.T. “Experimental Measurement of Heat Transfer Coefficients for Mixed Gas Working Fluids in Joule-Thomson Systems,” (Madison: Univ. of Wisc. Madison) MS [thesis] Available from: UW Madison Library System.